CHEMISTRY
A EUROPEAN JOURNAL

DOI: 10.1002/chem.200800731

Dipeptide-Based Low-Molecular-Weight Efficient Organogelators and Their Application in Water Purification

Sisir Debnath,[a] Anshupriya Shome,[a] Sounak Dutta,[a] and Prasanta Kumar Das*[a, b]

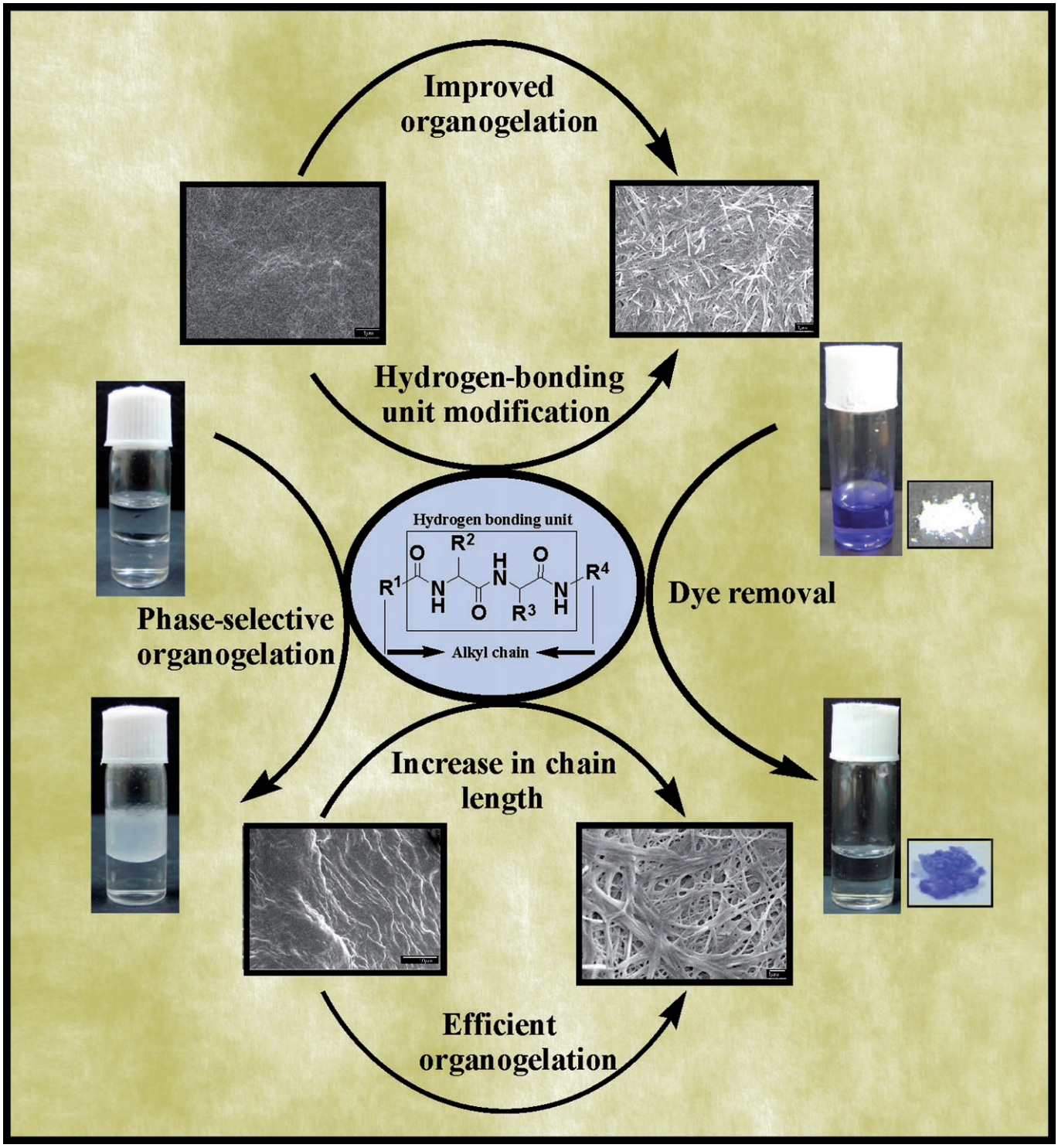

Abstract: The development of new low-molecular-weight gelators for organic solvents is motivated by several potential applications of gels as advanced functional materials. In the present study, we developed simple dipeptide-based organogelators with a minimum gelation concentration (MGC) of 6–0.15%, w/v in aromatic solvents. The organogelators were synthesized using different L-amino acids with nonpolar aliphatic/aromatic residues and by varying alkyl-chain length (C-12 to C-16). The self-aggregation behavior of these thermoreversible organogels was investigated through several spectroscopic and microscopic techniques. A balanced participation of the hydrogen bonding and van der Waals interactions is crucial for efficient organogelation, which can be largely modulated by the structural modification at the hydrogen-bonding unit as well as by varying the alkyl-chain length in both sides of the hydrophilic residue. Interestingly, these organogelators could selectively gelate aromatic solvents from their mixtures with water. Furthermore, the xerogels prepared from the organogels showed a striking property of adsorbing dyes such as crystal violet, rhodamine 6G from water. This dye-adsorption ability of gelators can be utilized in water purification by removing toxic dyes from wastewater.

Keywords: amino acids · dyes/pigments · organogels · peptides · supramolecular chemistry

Introduction

Low-molecular-weight organogelators are a family of small molecules that can immobilize organic solvents through molecular self-assembly, and thus represent a novel class of supramolecular materials.[1] A number of low-molecular-weight organogelators are known in the literature,[2–7] yet they continue to evoke intense interest because of their wide-ranging applications as templated materials, drug delivery agents, cosmetics, sensors, enzyme-immobilization matrices, as well as in phase selective gelation and water purification by dye adsorption.[8–11] These gelators create a three-dimensional (3D) network in organic solvents by self-organization of the monomeric species to higher-order structures, such as fibrous, tubular, or helical.[3e,f] Such self-assembling processes are driven by specific noncovalent intermolecular interactions, commonly electrostatic, dipole–dipole, van der Waals, π–π stacking, and/or hydrogen bonding.[12] Although intense effort has been devoted to establish a structure–property relationship for the development of low-molecular-weight gelators,[13] it is still difficult to predict the gelation ability of a compound. Thus, a major challenge in this field is the rational design of gelator molecules together with a proper understanding of the gelation mechanism.[14] It is also important to prepare gelators from eco-friendly, abundant precursors such as amino acids,[2,3] carbohydrates,[4] and lipids[5] that can be used as potent scaffolds. Amongst them, amino acid-based molecules are the most important because they are available in large quantities as cheap starting materials and synthetic methodologies are relatively simple and well established.

To this end, we recently reported the excellent water-gelation efficiency of cationic dipeptide amphiphiles.[15] A detailed structure–property study showed that the quaternary ammonium residue at the head group of the dipeptide amphiphiles (Scheme 1) plays a crucial role in hydrogelation. However, the precursor amine (Scheme 1) of this efficient hydrogelator (minimum gelation concentration (MGC) = 0.25%, w/v) was found to be a non-gelator both in water and organic solvents. The design of both organo- and hydrogelator from the same scaffold using simple synthetic methodology would be of great importance, however, such reports are rare, for example, that by Hanabusa and co-workers.[16]

Here, we found that incorporation of an alkyl chain at the N terminus of the precursor amine of the dipeptide amphiphile simply by coupling with long-chain carboxylic acid (Scheme 1) leads to the development of efficient organogelator (**1**) for aromatic solvents. Quaternization of the same amine with methyl iodide yielded a hydrogelator. It is quite established that an optimum balance between the hydrophilic and hydrophobic group is indeed essential to control both the hydrogen bonding and van der Waals interactions, the major driving forces for organogelation.[1a,2f] Hence, we have carried out a systematic investigation on the influence of different structural components of the dipeptide organogelators on their gelation efficiency (Scheme 2). The role of the dipeptide moiety was investigated using different L-amino acids of nonpolar aliphatic/aromatic residues (Scheme 3). Such structural alteration resulted in the development of two efficient organogelators **5** and **6** (Scheme 3), having L-phenylalanine–L-alanine and L-phenylalanine–glycine, respectively, as a hydrogen-bonding unit with MGC ≈0.15–0.4%, w/v in different aromatic solvents. To explore the role

[a] S. Debnath, A. Shome, S. Dutta, Dr. P. K. Das
Department of Biological Chemistry
Indian Association for the Cultivation of Science
Jadavpur, Kolkata 700032 (India)
Fax: (+91) 33-2473-2805
E-mail: bcpkd@iacs.res.in

[b] Dr. P. K. Das
Also at Centre for Advanced Materials
Indian Association for the Cultivation of Science
Jadavpur, Kolkata 700032 (India)

Supporting information for this article is available on the WWW under http://dx.doi.org/10.1002/chem.200800731: Generalized synthetic schemes for all the gelators, DSC curve for gelator **5**, 2D-NOESY spectra of **5** in $CHCl_3/C_6D_6$, and FTIR spectra of gelators.

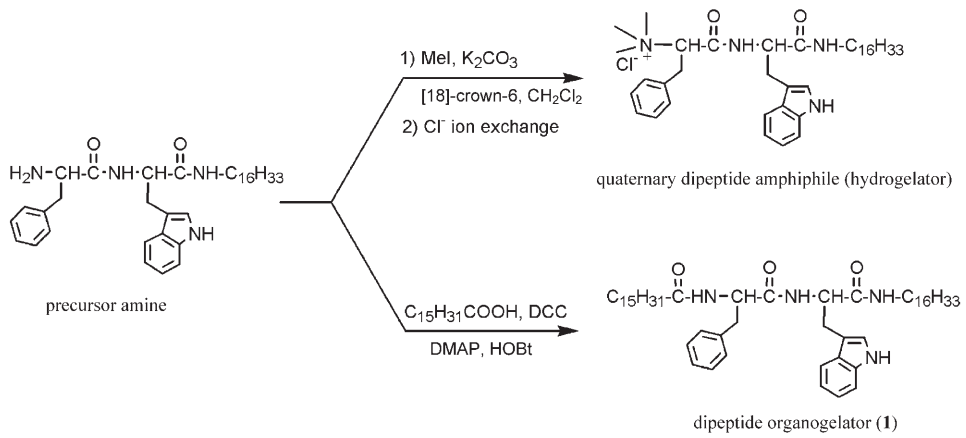

Scheme 1. Synthesis of organogel and hydrogel from the same precursor amine.

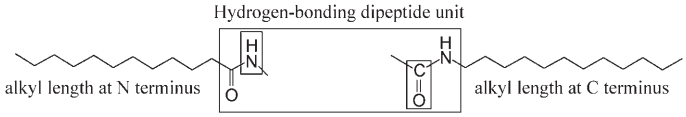

Scheme 2. Schematic representation of three different segments of the molecule.

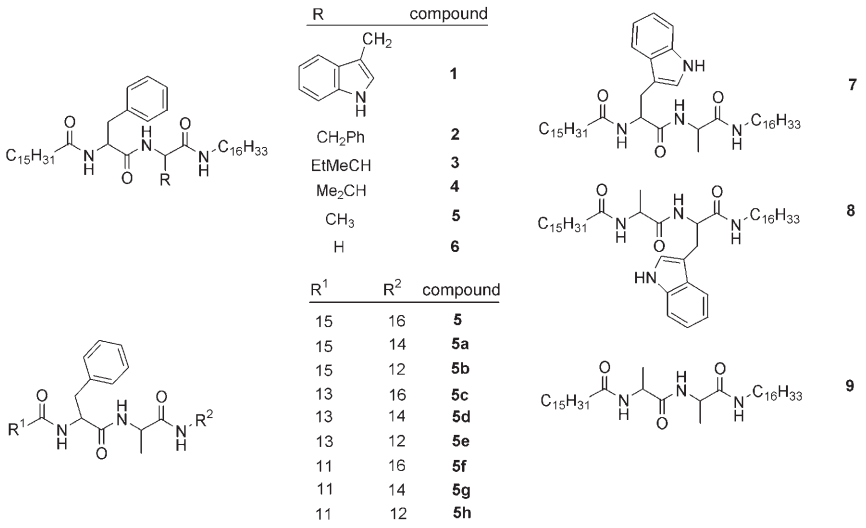

Scheme 3. Chemical structures of the compounds **1**–**9** and **5a**–**h**.

of the other important segment of the gelators, which has very occasional significance in organogelation, we altered the hydrophobic-chain length at both sides of the hydrogen-bonding unit of **5** from C-12 to C-16 (**5**, **5a**–**h**, Scheme 3). In general, the gelation efficiency increases as the alkyl-chain length increases, and the influence of the alkyl chain at the N terminus of the dipeptide is greater than that at the C terminus. Changes in the supramolecular arrangement of the organogels due to structural variation at the molecular level were investigated by using several spectroscopic and microscopic techniques. All dipeptide gelators showed selective gelation of oil (aromatic solvents) in the presence of water, which has tremendous implications for resolving problems such as oil spill. Strikingly, these organogelators posses an intriguing property of dye adsorption that can be suitably exploited in water purification.

Results and Discussion

Although low-molecular-weight organogelators have been known a long time,[17] studies on their structure–property relationship are intensifying toward the rational design and development of the self-aggregating low-molecular-weight gelators (LMWG).[1b,17,18] At the same time, the search is ongoing for a small molecule that can be used as an organogelator as well as a hydrogelator, or can be easily converted to both forms of gelator by a simple reaction/method.[3e,16] In this context, we recently reported a cationic dipeptide amphiphilic hydrogelator[15] (Scheme 1) comprising a quaternary ammonium residue at the head group, which plays an important role in its hydrogelation (MGC = 0.25 %, w/v). However, this amphiphile with a C-16 alkyl chain at the C terminus of the dipeptide did not show any organogelation ability, and also its precursor amine (Scheme 1) was found to be a non-gelator in both water and organic solvents. Hence, our aim was to transform this precursor amine to an organogelator by a simple modification, as the hydrogelator was prepared through a single-step quaternization (Scheme 1) from the same precursor. With this objective, *n*-hexadecanoic acid was coupled with the free amine (at the N terminus of the dipeptide) by a standard protocol (using dicyclohexylcarbodiimide (DCC) and 4-*N*,*N*-(dimethylamino)pyridine (DMAP), Scheme 1) that leads to the formation of a new dipeptide organogelator **1** (Scheme 3). The MGC of **1** in different aromatic solvents varies from 2.0–2.7 %, w/v (Table 1). However, it did not form gel in any other protic/aprotic non-aromatic solvents. It is well known that the gelation ability of the LMWGs depends largely on both the hy-

Table 1. Organogelation properties of **1–6** in organic solvents.

Solvent	Status of compounds[a] (MGC) [%, w/v]						
	1	**2**	**3**	**4**	**5**	**6**	**7**
toluene	TG (2.2)	TG (1.5)	TG (1.2)	TG (0.8)	TG (0.3)	TG (0.2)	TG (0.5)
tetralin	TG (2.0)	TG (1.3)	TG (1.0)	TG (0.7)	TG (0.25)	TG (0.15)	TG (0.6)
benzene	TG (2.1)	TG (1.5)	TG (1.2)	TG (0.8)	TG (0.3)	TG (0.2)	TG (0.8)
o-xylene	TG (2.2)	TG (1.5)	TG (1.2)	TG (0.8)	TG (0.3)	TG (0.2)	TG (0.6)
m-xylene	TG (2.2)	TG (1.5)	TG (1.2)	TG (0.8)	TG (0.3)	TG (0.2)	TG (0.6)
chlorobenzene	TG (2.4)	TG (1.3)	TG (1.2)	TG (0.6)	TG (0.3)	TG (0.2)	TG (0.5)
nitrobenzene	TG (2.6)	TG (1.6)	TG (1.5)	TG (0.7)	TG (0.4)	TG (0.2)	TG (0.8)
anisole	TG (2.7)	TG (1.7)	TG (1.4)	TG (0.5)	TG (0.4)	TG (0.3)	TG (0.7)
THF	S	S	S	S	S	S	S
DMSO	P	P	OG (0.9)	OG (0.7)	P	P	P
methanol	P	P	P	P	P	P	P
ethanol	P	P	P	P	P	P	P
isopropanol	P	P	P	P	P	P	P
1-butanol	P	P	P	P	P	P	P
1-hexanol	P	P	P	P	P	P	P
hexane	P	P	P	P	P	P	P
isooctane	P	P	P	P	P	P	P
water	I	I	I	I	I	I	I
chloroform	S	S	S	S	S	S	S
DMF	P	P	P	P	P	P	P

[a] TG, transparent gel; OG, opaque gel; P, precipitate; S, solution; I, insoluble.

drophilic and hydrophobic parts of the molecules.[2f] In the present case, the organogelator (**1**) has three regulatory segments responsible for its self-aggregation: 1) a hydrophobic tail at the N terminus of the dipeptide, 2) a hydrophobic tail at the C terminus of the dipeptide, and 3) a hydrogen-bonding dipeptide unit at the middle of molecule (Scheme 2). Thus, to understand the influence of the different parts of the synthesized molecules in organogelation, we systematically varied the each segment of the gelator (Scheme 2).

At first, structural variation was performed at the central hydrogen-bonding unit by changing L-amino acids with nonpolar aliphatic/aromatic residues. While keeping the amino acid at the N terminus fixed, that is, L-phenylalanine, and also the hydrophobic chain of 16 carbon atoms at the two ends, we substituted the C-terminal amino acid in **1** (L-tryptophan) by L-phenylalanine (**2**), L-isoleucine (**3**), L-valine (**4**), L-alanine (**5**), and glycine (**6**, Scheme 3). To evaluate their gelation abilities, the required amount of compound was heated in a given solvent until the solid was completely dissolved. The homogenous solutions were then cooled slowly to room temperature and gelation was observed visually after one hour. The "stable-to-inversion of the container" method was used to confirm gelation, that is, if a gel did not show any gravitational flow over a period of several hours. This process was repeated to confirm the thermoreversibility of the gelation process. A series of organic solvents was used to test the gelation behavior. In concurrence with the gelation behaviour of **1**, all other compounds are either insoluble or precipitated out in all other protic/aprotic non-aromatic solvents, except for THF and chloroform, in which these compounds are soluble (Table 1). As expected, the molecules are also insoluble in water. However, all the compounds formed stable transparent gels in a wide range of aromatic solvents, and **3** and **4** also yielded opaque gels in DMSO (Table 1). All these gels were quite stable at room temperature for several months. Interestingly, the gelation ability in aromatic solvents was largely dependent on the amino acid substitution at the C terminus (Scheme 2). On the whole, the MGC decreased by almost an order magnitude from $2.4\pm0.4\,\%$, w/v to $0.2\pm0.1\,\%$, w/v as the size of the side-chain substitution from **1** (L-tryptophan) to **6** (glycine) steadily decreased, irrespective of the nature of the aromatic solvents (Table 1). Furthermore, the gelation efficiency for any individual dipeptide did not vary to a significant extent in different aromatic solvents. Compounds **5** and **6**, with the smaller side-chain-substituted amino acids L-alanine and glycine, respectively, were found to be the most efficient organogelators (MGC$\approx$0.2 and 0.3%, w/v, respectively). A decrease in the gelation efficiency as the size of the side-chain residue at the hydrogen-bonding unit increases is also consistent with previous observations by Luo et al.,[2f] in which an amphiphile lost its gelation ability due to alteration from L-alanine to L-phenylalanine at the head group. This is probably due to the increase in steric hindrance from **6** to **1** by the side-chain substitution at the hydrogen-bonding site that weakens the essential intermolecular hydrogen bonding between the neighboring molecules for gelation. Increase in the size of the substituted side chain at the N-terminal amino acid also moderately reduced the gelation efficiency. The MGC increased almost two-fold from $\approx$0.3 to $\approx$0.6%, w/v (Table 1) in different aromatic solvents from **5** to **7** in which L-phenylalanine at the N terminus was replaced with L-tryptophan, keeping all other segments intact, as in gelator **5**.

So far from **1** to **6**, we have altered the amino acids at the C terminus that showed increase in gelation efficiency as the size of the side-chain residue of the amino acids decreased. However, fixing the C terminus (L-tryptophan) in organogelator **1** and decreasing the amino acid size at the N terminus from L-phenylalanine to L-alanine yielded another organogelator (**8**). Although the MGC (1.4%, w/v) of **8** in toluene is less than that of **1** (2.2%, w/v, Table 1), the improvement in gelation efficiency is not as dramatic as that obtained by altering the amino acid at the C terminus (MGC of **5**= 0.3%, w/v). Because a smaller side-chain residue of amino acids at both the N and C termini improved the gelation efficiency, we synthesized compound **9** with L-alanine at both termini, with the expectation of a further decrease in MGC. However, **9** did not show any gelation ability and was insoluble in different aromatic solvents. Thus, presence of an

aromatic side-chain residue at either of the termini of the hydrogen-bonding unit may be essential for gelation.

The influence of the other two segments (hydrophobic part at both ends of the dipeptide, Scheme 2) on the gelation efficiency was tested by using one of the most efficient organogelators, **5**, by varying the alkyl-chain length from 12 to 16 carbon atoms (**5**–**5h**, Scheme 3). All these structural variants at both hydrophobic ends also yielded transparent organogels in different aromatic solvents (Table 2). If the alkyl-chain length was kept constant at C-12, C-14, or C-16 carbon atoms at the N terminus (R^1, including carbon atoms of −C=O, Scheme 3), a decrease in hydrophobic-chain length at the C terminus (R^2, Scheme 3) from 16 to 12 carbon atoms led to a modest decrease in gelation efficiency of about 1.5–2.5-fold (Table 2). For example, in xylene, in which R^1 = C-16, with variation of R^2 from 16 to 12 (**5**, **5a**, **5b**, respectively), the MGC increased two-fold from 0.3–0.6%, w/v. Similarly, the variation of R^2 from 16 to 12 (**5c**, **5d**, **5e**, respectively), led to an increase in MGC of 1.5-fold from 0.9–1.3%, w/v if R^1 = C-14, whereas the increase in MGC was 2.2-fold from 2.5–5.5%, w/v for **5f**, **5g**, **5h**, respectively, if R^1 = C-12. However, the alteration in MGC values was quite significant, ≈7–10-fold if the R^2 was kept constant and the R^1 was varied from 12–16 carbon atoms. The MGC increased ten-fold (0.3–3.0%, w/v) as R^1 decreased from 16–12 carbon atoms in benzene in the case of **5** to **5c** to **5f** in which R^2 = C-16. Similar trends were observed for **5a**, **5d**, **5g** and **5b**, **5e**, **5h**, for which R^2 = C-14 and C-12, respectively, and R^1 varied from C-12 to C-16. Hence, the preceding results clearly delineate that the hydrophobic chain at the N terminus has a greater influence on the gelation efficiency of these dipeptides than that at the C terminus. By considering all the structural variations, including the hydrogen-bonding unit and alkyl-chain length at both its ends, the gelation efficiency can be improved even up to 30-fold from 6%, w/v for **5h** to 0.2%, w/v for **6**.

Table 2. Minimum gelation concentration (MGC) of **5**, **5a**–**5h** in aromatic solvents.

Solvent	MGC [%, w/v]								
	5	**5a**	**5b**	**5c**	**5d**	**5e**	**5f**	**5g**	**5h**
toluene	0.3	0.5	0.7	1.0	1.25	1.4	2.5	4.0	5.5
tetraline	0.25	0.4	0.55	0.85	1.1	1.1	2.0	3.5	5.0
benzene	0.3	0.5	0.75	1.1	1.3	1.5	3.0	4.2	6.0
o-xylene	0.3	0.4	0.6	0.9	1.2	1.3	2.5	3.9	5.5
m-xylene	0.3	0.4	0.6	0.9	1.2	1.3	2.5	3.9	5.5
chlorobenzene	0.3	0.4	0.6	0.9	1.3	1.4	2.4	4.0	5.2
nitrobenzene	0.4	0.5	0.8	1.1	1.3	1.6	2.7	4.3	5.4
anisole	0.4	0.6	0.8	1.0	1.4	1.5	2.7	4.2	5.3

Thermoreversible organogels melt upon slow heating and turn to gel on cooling. The gel-to-sol transition temperature (T_{gel}) of the gelators having different amino acids (**1**–**6**) and different chain lengths (**5d** and **5h** were taken as representative examples) were almost comparable at their MGC, only that for **5** was slightly lower (Figure 1). In concurrence with the literature, T_{gel} increased as gelator concentration increased.[12a,f,19] The observed T_{gel} value (48 °C, Figure 1) at 0.7%, w/v for **5** determined by following the gravitational flow of the liquid from the gel was in concurrence with the value that was obtained from differential scanning calorimetric (DSC) data (45.1 °C) for the same gelator (See Supporting Information, Figure S1). The gel-to-sol melting transition was less sharp than the sol-to-gel cooling transition, and also the corresponding temperature (17 °C) was lower than that of T_{gel}. Such a hysteresis behaviour of low-molecular-weight gelators is well known in the literature.[3e,19a,20] The preceding observations indicate the influence of amino acid constituent and alkyl-chain-length-induced hydrophobicity in the supramolecular association of the individual monomer in the 3D network of the gels.

Microscopy studies: To get a visual insight into the morphology of organogels, the supramolecular 3D network was inspected by field emission scanning electron microscopy (FESEM). All the xerogels prepared from toluene showed a clear fibrous network at their MGC (Figure 2). However, the differences in size and nature of the fibers were dependent on the constituent of the hydrogen-bonding unit and the length of its two hydrophobic ends. Gelators **1**–**3**, with bigger side-chain substitution and also higher MGC, exhibited an interconnected network of thin fibrils with a thickness of a few tens of nanometers (20–40 nm, Figure 2a–c). In **4**, having a shorter side chain, an intertwined 3D network was observed in which two or more fibers were associated with each other to form a thicker fiber of ≈60–80 nm (Figure 2d). As reflected in the MGC values (Table 1), the efficient gelators **5** and **6**, with a smaller substituent at the site of the hydrogen-bonding unit, formed an entangled 3D ag-

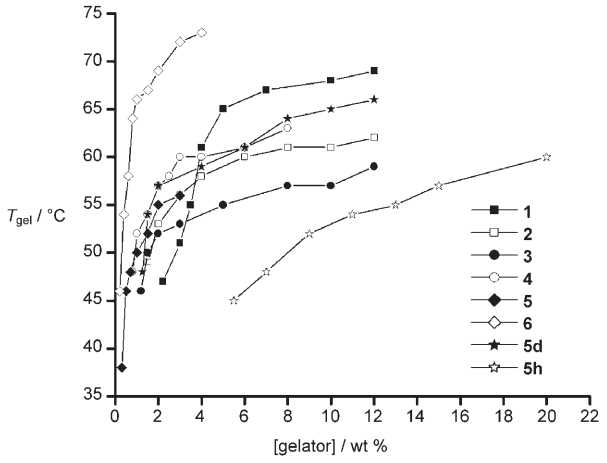

Figure 1. Plot of gel-to-sol transition temperature (T_{gel}) against gelator concentration.

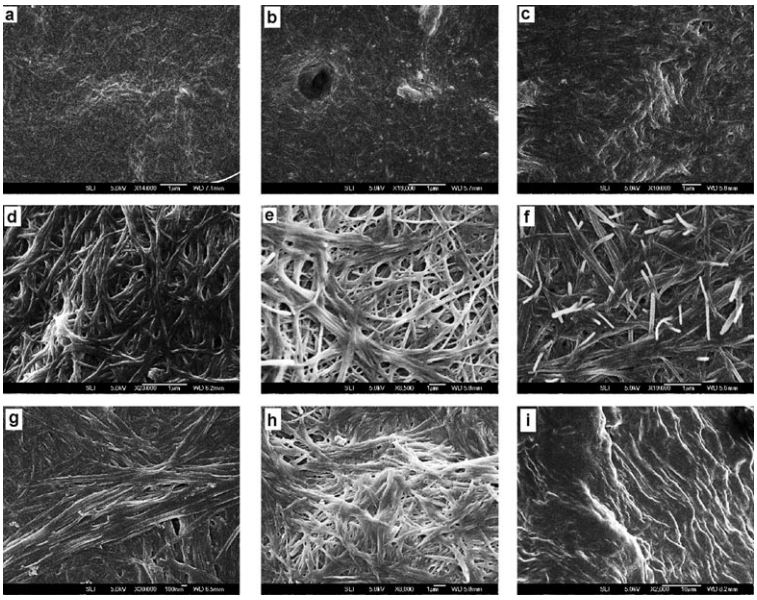

Figure 2. a)–i) FESEM images of dried samples of **1**–**7**, **5d**, and **5h**, respectively, at MGC.

gregate with fibers of 160–180 and 80–120 nm thick (Figure 2e and f), respectively, probably due to the lower steric hindrance resulting in effective intermolecular hydrogen bonding. Such entangled fibrous networks possibly facilitate the entrapment of more solvent molecules and also prevent the flow of solvent molecules.[21] Therefore, as the size of the amino acid side-chain substitution at the hydrophilic residue decreased from **1** to **6**, the intermolecular hydrogen bonding strengthens, increasing the thickness of the fibers, which may account for the better gelation in the same order. A similar intertwined fibril network was observed in the case of **7** (Figure 2g), with fiber thickness of ≈70 nm and MGC = 0.5 %, w/v. Thus, the above observation clearly indicates that the hydrogen-bonding unit plays a crucial role in dictating the self-aggregation of the organogels, as well as its morphology, as reflected in the SEM images. Furthermore, the influence of the hydrophobic region on the gelation behavior was investigated by taking SEM images of **5**, **5d**, and **5h** having 16, 14, and 12 carbon atoms at both the sides of hydrogen-bonding unit, respectively. Compounds **5** and **5d** (Figure 2h) showed almost similar morphology and comparable fiber thickness. However, in case of **5h**, the MGC increased significantly to 5.5 %, w/v in toluene, presumably due to the loosely packed, thin parallel fibers of 30–40 nm (Figure 2i). This observation corroborates the fact that the gelation ability gradually decreases as the alkyl-chain length of the dipeptide gelator decreases.

The morphology of the xerogels was further confirmed from the atomic force microscopy (AFM) of an efficient gelator, **5**. The AFM image (Figure 3a) supports the entangled fibril structure of the xerogels in which the diameter of every fiber (≈180 nm) was comparable to that observed in the corresponding SEM image of **5** (Figure 2e). Magnification of the fibers showed that each fiber was formed by the helical orientation of several small fibers (Figure 3b). Furthermore, transmission electron microscopy (TEM) of **5** at a lower concentration than MGC (Figure 3c) showed similar intertwined fibers of ≈80 nm thickness, which possibly become associated with each other to form a thicker fiber of ≈160–180 nm at MGC.

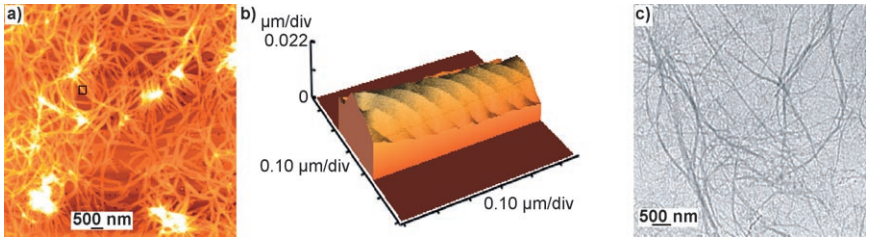

Figure 3. a) AFM image of **5** at MGC (0.3 %, w/v); b) 3D view of region marked in image a); c) TEM image of dried sample of **5** prepared from toluene.

^{1}H NMR experiments: ^{1}H NMR spectroscopy is a powerful tool to study the hydrogen-bonding interaction in self-assembled aggregation.[12b–d,22] It is well known that hydrogen bonding is one of the major driving forces in organogelation for low-molecular-weight gelators,[1a] which is also evident from the preceding results. Thus, to get a quantitative idea of the orientation of the gelator molecule in the self-assembled 3D network due to the hydrogen-bonding interactions at the molecular level, a systematic temperature-dependent NMR study was performed using 1 %, w/v of **5** in C_6D_6. All the amide protons (H_a, H_b, H_c, Figure 4) showed weak and broad NMR signals at $\delta = 5.9$, 5.5, and 5.1 ppm, respectively, at 25 °C. As temperature increased to 45 °C, the peak nature did not change significantly because the compound was still in the gel state, however, the amide protons notably upfielded to $\delta = 5.6$, 5.2, and 4.8 ppm for H_a, H_b, H_c, respectively. As the temperature exceeded the T_{gel} (50 °C, Figure 1) of **5** at 1 %, w/v, the intermolecular hydrogen bonding is presumably destroyed leading to the transition from gel to sol (non-self-assembled species) at 55 and 65 °C. At these temperatures the spinning nuclei showed their characteristic stronger and sharper signals, as in solution (Figure 4). In addition, the amide protons further shielded to $\delta = 5.1$, 4.82, and

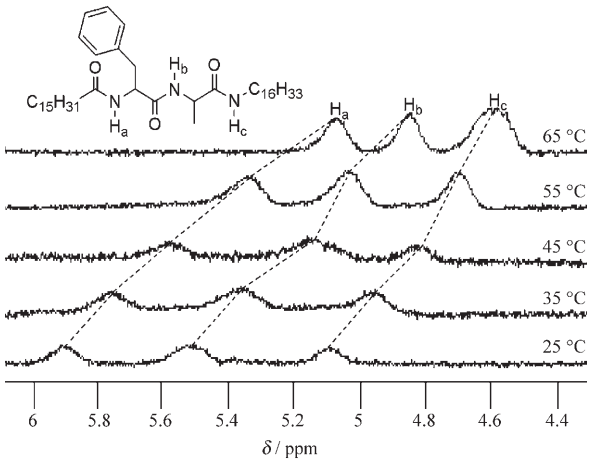

Figure 4. Change in ^{1}H NMR chemical shift of three amide protons of gelator **5** (1%, w/v) in C_6D_6 as temperature increases from 25 to 65 °C.

4.55 ppm, respectively. However, the broadening and decrease in intensity of NMR peaks at low temperature is probably due to the restricted motion of these protons in self-aggregated gel. These results implied that the intermolecular hydrogen bonds were present between the neighboring amide groups through a −C=O···H−N− linkage in the gel state at room temperature. The observed upfield shift of amide protons with an increase in temperature is due to the breaking of intermolecular hydrogen bonds that leads to gel-to-sol transition.[12d]

We further investigated the possible intermolecular interactions between gelator and its neighboring molecules by performing 2D NOESY experiments with **5** (1%, w/v) in $CDCl_3$ and also in the presence of 50% C_6D_6. As expected, no off-diagonal cross-peak was observed for the nongelated state of the amphiphiles in $CDCl_3$. However, at 50% C_6D_6 content, in which the self-assembling process has already initiated towards gelation, off-diagonal cross-peaks were observed between methylene protons of the hydrophobic long chain and the aromatic protons as well as with chiral proton of the C-terminal amino acid L-alanine (See Supporting Information, Figure S2). This observation specifies that an interaction exists through space between the protons of the central hydrophilic residue and the hydrophobic alkyl-chain protons, which also plays a possible role in organogelation.

FTIR spectroscopy: FTIR is another powerful tool for studying hydrogen bonding in the self-assembly of gelators.[3e,f,12e,g,21,23] FTIR spectra of xerogels (prepared from toluene) and the non-self-assembled state of these gelators in $CHCl_3$ were recorded (Figure 5a, Supporting Information Figures S3, S4) by using a Nicolet Magna IR-750-series-II spectrophotometer. The FTIR spectrum in chloroform of compounds **1**–**6**, **5d**, and **5h** (shown as representative examples of varying chain length) showed transmission bands at 3431–3440, 1659, and 1512–1519 cm^{-1}, which are characteristic of non-hydrogen-bonded νN−H (amide A), νC=O (amide I), and δN−H (amide II) frequencies, respectively.[2f,3f,12e] On the other hand, the transmission band of the corresponding xerogel appeared at 3290–3308, 1631–1639, and 1544–1551 cm^{-1}, respectively. These are the characteristic transmissions of the intermolecular hydrogen-bonded amide group (Figure 5a).[2f,3e] The observed frequencies in xerogel are always lower for the νN−H (amide A) and C=O stretching band (amide I), and higher for the N−H bending band (amide II) than for that in $CHCl_3$. Again, the transmission band of the (ν_{as}) and symmetric (ν_s) CH_2 stretching frequencies of the above-mentioned compounds appeared at 2928 and 2855 cm^{-1}, respectively, in chloroform solution,

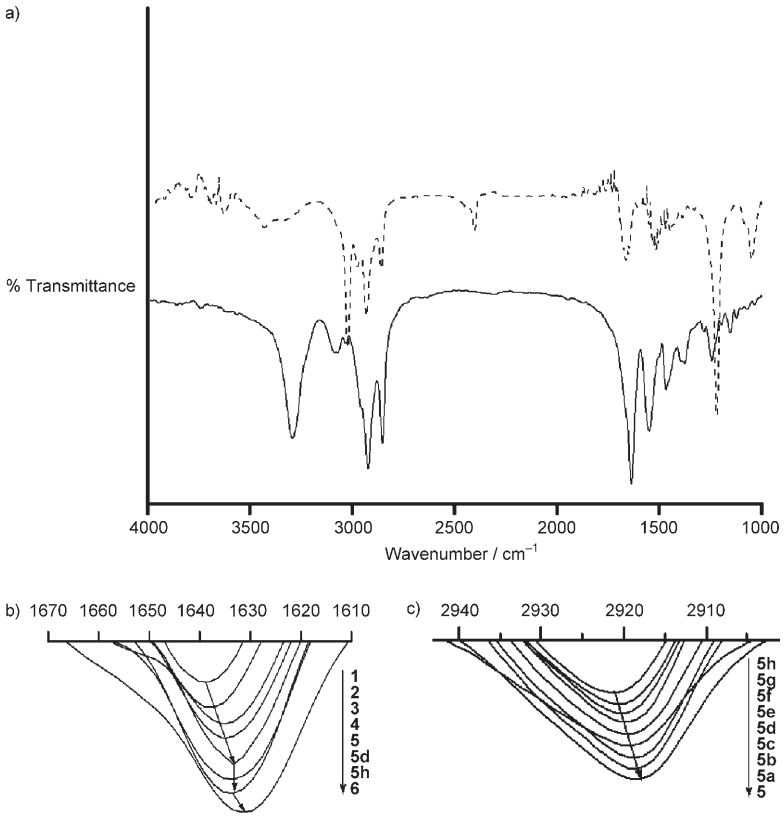

Figure 5. a) FTIR spectra of gelator **5** in $CHCl_3$ (dashed line) and xerogel (solid line) obtained from toluene. b) FTIR spectra of C=O stretching frequency of **1**–**6**, **5d**, and **5h**. c) FTIR spectra of antisymmetric (ν_{as}) CH_2 stretching frequency of **5**–**5h**.

whereas they shifted to 2919 and 2850 cm^{-1}, respectively, in the gel state. In concurrence with previous reports, this shift in wavenumber of antisymmetric (ν_{as}) and symmetric (ν_s) CH_2 stretching frequencies indicates the decrease in fluidity of the hydrophobic chains due to strong aggregate formation of the alkyl chain through van der Waals interactions.[21] Hence, the main factors responsible for the organogelation of the above compounds are hydrogen bonding and van der Waals interactions. In Figure 5b we have tried to establish a correlation between the organogelation efficiency and hydrogen-bonding unit through a comparative data analysis of C=O stretching frequency with the varying amino acids at the hydrophilic residue. Xerogel of gelator **1** to **6** showed a steady decrease in C=O stretching frequency (1639, 1637, 1635, 1634, 1633, 1631 cm^{-1}) that remained almost constant at 1659 cm^{-1} in their non-self-assembled chloroform solution. The observed decrease in amide-I band frequency is presumably due to the increasing strength of the hydrogen bond yielding improvement in the gelation efficiency. Thus, the decrease in MGC values (Table 1) as the size of the amino acid side-chain substitution decreases from **1** to **6** is primarily due to the increase in the hydrogen-bonding ability in the same order. The strength of hydrogen bonding depends on the constituent of the amino acid present at the hydrophilic residue. This was further confirmed by comparing the stretching frequency of the amide I band of **5**, **5d**, and **5h**. These three gelators posses the same amino acid constituted hydrogen-bonding unit. As a consequence, they showed a similar stretching frequency of the C=O bond at 1633 cm^{-1} (Figure 5b). However, they showed differences in gelation ability, possibly due to the variation in their hydrophobic alkyl-chain length. We attempted to correlate this by comparing the antisymmetric (ν_{as}) and symmetric (ν_s) CH_2 stretching frequencies of the xerogels **5h** to **5**. We found that the transmission band of antisymmetric (ν_{as}) CH_2 stretching frequency decreased from 2921.5 to 2918.5 cm^{-1} for xerogels **5h** to **5** as the chain length increased (Figure 5c). A similar but very minute shift was also found for the transmission band of symmetric (ν_s) CH_2 stretching frequency from 2851.5 to 2850 cm^{-1} for **5h** to **5**. Such a small but definite shift probably arises from better hydrophobic packing with longer alkyl chain, leading to superior gelation efficiency and lower MGC. An increase in intensity of the methylene scissoring vibration δ (CH_2) band $\approx$1464 cm^{-1} with an increase in the alkyl-chain length indicates the high *trans* conformational packing of alkyl chain leading to the superior gelation efficiency in **5**.[24]

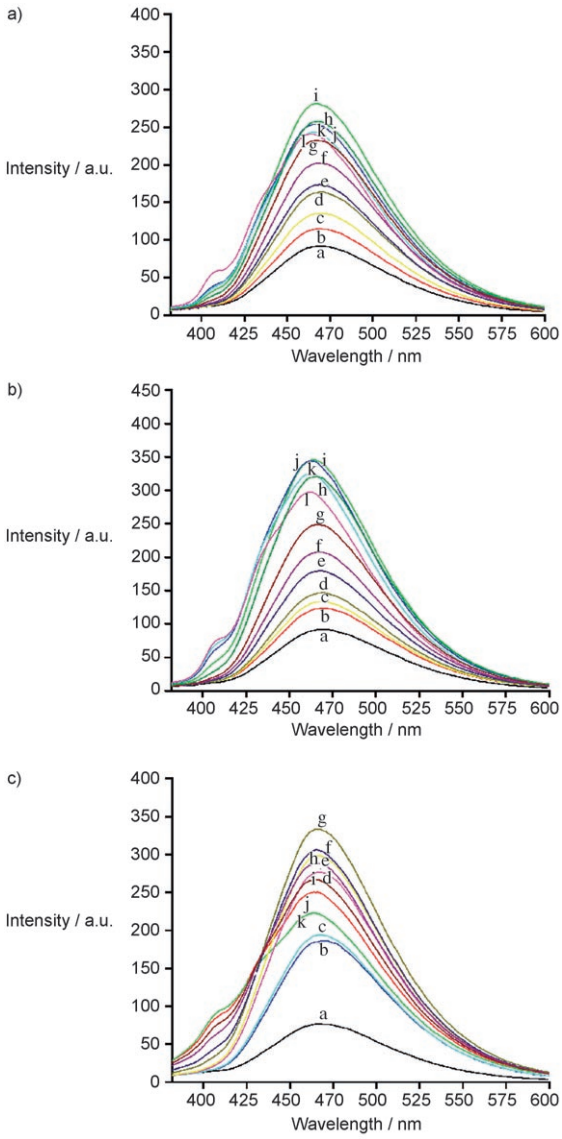

Figure 6. Luminescence spectra of ANS (1×10^{-5} M) in response to varying concentrations of gelator **5** (a), **5d** (b), and **5h** (c) in toluene at RT. [**5**] (%, w/v) a=0; b=0.0025; c=0.005; d=0.01; e=0.025; f=0.05; g=0.075; h=0.1; i=0.25; j=0.5; k=1; l=2. [**5d**] (%, w/v) a=0; b=0.0025; c=0.005; d=0.01; e=0.025; f=0.05; g=0.01; h=0.25; i=0.5; j=1; k=1.5; l=2. [**5h**] (%, w/v) a=0; b=0.005; c=0.01; d=0.05; e=0.1; f=0.5; g=1; h=2; i=4; j=6; k=8.

Luminescence study: Van der Waals, as well as hydrophobic interactions, during the supramolecular association of individual molecules, as observed in the preceding FTIR studies, were further investigated by taking luminescence spectra of 8-anilino-1-naphthalene-sulphonic acid (ANS), a hydrophobic fluorescent probe, during gelation of **5**, **5d**, and **5h** in toluene (Figure 6). The intensity of ANS gradually increased as the concentration of gelators increased at almost a fixed emission wavelength (λ_{em}) of $\approx$468 nm. The observed steady increase in intensity up to a concentration 4–10 times lower than the MGC showed its propensity to aggregate as hydrophobicity increases, leading to the formation of fibers, as seen in microscopy studies. As the concentration of gelators increased further, the ANS intensity remained almost constant up to MGC. Above MGC, a slight decrease in emission intensity was observed, along with a small blue shift up to 460 nm. This blue shift may arise due to formation of a more hydrophobic environment by the long hydrophobic ends of the gelator. In addition, a new emission peak at 415 nm was generated above MGC, which may be due the

peptide-bound ANS, whereas the peak at 460 nm is due to the fluorescence of free ANS.[25]

Selective organogelation from oil/water: The phase-selective gelation from a given mixture of solvents is always a daunting task that becomes more challenging if one of the solvents is water. To this end, Bhattacharya and Ghosh reported the "first phase-selective gelation of oil from oil/water mixtures", which has tremendous implications for the dissolution of an oil spill.[10] Interestingly, organogelators in the present study were found to be suitable for selective gelation of an oil (aromatic solvent) from an oil/water mixture due to their insolubility in water and good organogelation abilities in many aromatic solvents. In a typical procedure, 1 mL of toluene and 1 mL of water were mixed in a sample tube to which 10 mg of gelator **5** was added (Figure 7a). The gelator **5** was then solubilized in this two-phase solution by heating and also shaken vigorously to ensure homogeneous dispersion of oil in water (Figure 7b). After cooling the mixture to room temperature, the toluene layer was gelated, and the water layer remained intact in liquid state (Figure 7c). Next, the organogel was separated from the water simply by filtration. The same observation was found to be true for all other organogelators (Scheme 3, Table 1) and also in other aromatic solvents.

Dye-adsorption study: Removal of toxic dyes from wastewater is an important research front for obvious environmental reasons. Organic–inorganic hybrid gels have been shown to remove different toxic dyes and pollutants from water, besides the conventional use of activated charcoal, clay, porous silica, different polymers, recently polymeric organogel scaffold.[11] Ideally, dye-adsorbing agents should have both hydrophilic and hydrophobic domains for efficient dye removal. As preceding studies have shown that the present organogelators have both desired domains in their supramolecular association, we thought of exploiting these gels in water purification. To this end we used the xerogels (prepared from toluene) of the gelators **1**–**7** for dye adsorption. Following submergence of the xerogel (10 mg) of **5** into aqueous solutions of dyes, it efficiently adsorbed the dye molecules from water over a period of time (Figure 8). After 24 h, more than 97% of crystal violet was removed by the adsorbent. Adsorption of dye from aqueous solution was monitored by UV-visible spectroscopy (Figure 8a), which revealed (inset, Figure 8a) that the entire dye molecule was transferred from water to xerogel leaving clear water. The ability of other organogelators (**1**–**4**, **6**, **7**) to adsorb crystal violet was similarly monitored (Figures S5, S6). The maximum amount of dye adsorption and the time required are largely dependent on the molecular architecture of the gelators. Compounds **1** and **7**, having a tryptophan moiety as one of the dipeptide units, were most efficient for the adsorption of dyes. The maximum amount of crystal violet was adsorbed by gelators **1** and **7**, 21.7 and 14.3 $mg\,g^{-1}$, respectively, whereas for the other gelators this amount is only 4–9 $mg\,g^{-1}$ (see Supporting Information, Table S1). Furthermore, these two gelators took only 10 and 15 h, respectively, for the complete adsorption of the dye. The FESEM image of crystal violet entrapped in xerogel of **5** (Figure 8b) clearly showed the presence of dye particles (white dots) on the nanofibrillar network of the gel. Adsorption of rhodamine 6G (Figure 8c) was also investigated by UV-visible spectroscopy using **1**, **5**, and **7** (Figure S7, Supporting Information). The maximum amounts of dye adsorption for **1** and **7** are 13.1 and 9.4 $mg\,g^{-1}$, respectively (Table S1, Supporting Information). However, the xerogels took longer to adsorb rhodamine 6G than crystal violet.

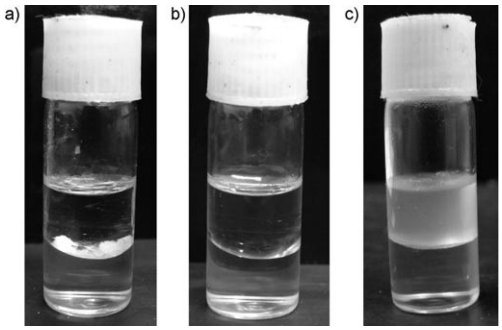

Figure 7. a) 1 mL toluene and 1 mL water together with 10 mg of gelator **5**. b) Gelator **5** was dissolved by heating. c) Selective gelation of toluene layer by **5** at RT.

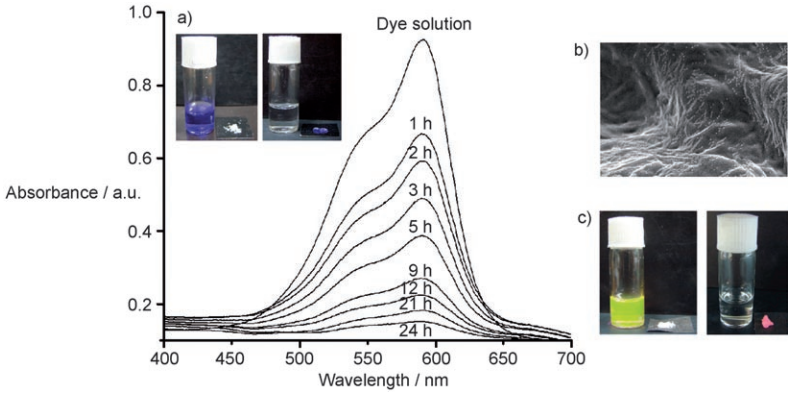

Figure 8. a) UV/Vis spectrum of aqueous solution of dye (crystal violet) indicating the time-dependent adsorption of the dye from water by xerogel of **5**. Inset: photograph of crystal violet adsorption from water by xerogel of **5**. b) SEM image of crystal violet adsorbed by xerogels of **5**. c) Photograph of rhodamine 6G adsorption from water by xerogel of **5**.

Conclusion

Although considerable attention has been paid to find a possible structure–activity correlation of the low-molecular-weight organogelators, some questions remain unanswered. Thus, a better understanding of these systems is required. The present study contributes to this line of research because we showed that rational designing can yield both organo- and hydrogelator from the same scaffold by using a simple synthetic methodology. We systematically analyzed the organogelation properties of a series of dipeptide amphiphiles, with special emphasis on the structural aspects, as well as the mechanism of the gelation processes. The gelation process was analyzed at the molecular level to explain how minute changes in the chemical structure influence the self-assembling behavior. We have established a relationship between the different structural components of gelator and their organogelation efficiencies. Interestingly, these organogelators gelate selectively aromatic solvents from their mixtures with water. Also, the xerogels could find potentially significant applications in wastewater treatment as they showed an intriguing property of adsorbing dyes from water. Furthermore, our ongoing research on the application of these organogelators in nanobiotechnology should further expand the application of these soft materials.

Experimental Section

All amino acids, *n*-dodecylamine, *n*-hexadecylamine, *n*-dodecanoic acid, *n*-tetradecanoic acid, *n*-hexadecanoic acid, dicyclohexylcarbodiimide (DCC), 4-*N*,*N*-(dimethylamino) pyridine (DMAP), 1-hydroxybenzotriazole (HOBT), and solvents were procured from SRL (India). 1,1′-Carbonyldiimidazole (CDI) was purchased from Spectrochem, India. All deuteriated solvents for NMR experiments, 8-anilino-1-naphthalene-sulphonic acid (ANS), and *n*-tetradecylamine were obtained from Aldrich. Thin layer chromatography was performed using Merck precoated silica gel 60-F_{254} plates. ^{1}H NMR spectra were recorded by using an AVANCE 300 MHz (Bruker) spectrometer. Mass spectrometric data were acquired by the electron spray ionization (ESI) technique by using a Q-tof-micro Quadruple mass spectrometer (Micromass). The specific rotations of the synthesized compounds were measured by using a Perkin–Elmer (model 341LC) polarimeter.

Synthetic procedures: All the dipeptide organogelators were synthesized following a standard peptide chemistry as shown in Scheme S1 (Supporting Information). Briefly, *tert*-butyloxycarbonyl (Boc)-protected L-amino acid was coupled with *n*-alkylamine by using CDI (1 equiv) in dry dichloromethane (DCM). The pure Boc-protected amide was then obtained through column chromatography by using 60–120 mesh silica gel and ethyl acetate/hexane as eluent. The product was subjected to deprotection by trifluoroacetic acid (TFA, 2 equiv) in dry DCM. After 2 h of stirring, solvents were removed with a rotary evaporator, and the mixture was added to ethyl acetate. The EtOAc part was thoroughly washed with aqueous 10% sodium carbonate solution followed by brine to neutrality. The organic part was dried over anhydrous sodium sulfate and concentrated to get the corresponding amine. This amine was then coupled with another Boc-protected L-amino acid by using CDI (1 equiv) in dry DCM. The purified product was obtained by column chromatography using 60–120 mesh silica gel and ethyl acetate/toluene as eluent. The product was again subjected to deprotection by trifluoroacetic acid (TFA, 2 equiv) in dry DCM, as described above, to get the corresponding amine. The final product was obtained by another coupling reaction using this amine and the required long-chain acid by CDI (1 equiv) in dry DCM. The final product was insoluble in DCM and hence the pure product was simply filtered and thoroughly washed with an excess amount of DCM. For **1**, **7**, and **8** the coupling steps were performed using DCC, DMAP, and HOBT instead of CDI (see Supporting Information, Scheme S1).

Data for 1: $[\alpha]_D^{20} = -35°$ ($c = 1.2$ in $CHCl_3$); ^{1}H NMR (300 MHz, $CDCl_3$, 25 °C, TMS): $\delta = 8.12$ (s, 1H), 7.4–6.94 (m, 10H), 6.33–6.31 (d, 1H), 5.92 (t, 1H), 5.6–5.58 (d, 1H), 4.69–4.67 (m, 1H), 4.52–4.5 (m, 1H), 3.47–3.41 (m, 2H), 3.16–2.94 (m, 4H), 1.72–1.69 (m, 2H), 1.48–1.47 (br, 2H), 1.39–1.07 (br, 52H), 0.9–0.81 ppm (m, 6H); ESI-MS: *m*/*z*: calcd for $C_{52}H_{84}N_4O_3$: 812.6543 [M^+]; found: 835.7579 [M^++Na]; elemental analysis calcd (%) for $C_{52}H_{84}N_4O_3$: C 76.80, H 10.41, N 6.89: found: C 76.58, H 10.18, N 6.86.

Data for 2: $[\alpha]_D^{20} = -18.5°$ ($c = 6.1$ in $CHCl_3$); ^{1}H NMR (300 MHz, $CDCl_3$, 25 °C, TMS): $\delta = 7.31$–6.97 (m, 10H), 6.59–6.56 (d, 1H), 6.04–6.02 (d, 1H), 5.88 (t, 1H), 4.64–4.56 (m, 1H), 4.44–4.42 (m, 1H), 3.14–2.87 (m, 6H), 2.16–2.04 (m, 2H), 1.51–1.43 (m, 2H), 1.32–1.25 (br, 52H), 0.89–0.85 ppm (m, 6H); ESI-MS: *m*/*z*: calcd for $C_{50}H_{83}N_3O_3$: 773.6434 [M^+]; found: 796.7031 [M^++Na]; elemental analysis calcd (%) for $C_{50}H_{83}N_3O_3$: C 77.57, H 10.81, N 5.43; found: C 77.39, H 11.01, N 5.53.

Data for 3: $[\alpha]_D^{20} = -8.7°$ ($c = 6.7$ in $CHCl_3$); ^{1}H NMR (300 MHz, $CDCl_3$, 25 °C, TMS): $\delta = 7.27$–7.16 (m, 5H), 6.69–6.66 (d, 1H), 6.21–6.18 (d, 1H), 6.03 (br, 1H), 4.77–4.7 (m, 1H), 4.14–4.08 (m, 1H), 3.25–3.16 (m, 2H), 3.13–2.99 (m, 2H), 2.15 (t, 2H), 1.54–1.46 (m, 5H), 1.24 (br, 52H), 0.89–0.82 (m, 9H), 0.69–0.68 ppm (t, 3H); ESI-MS: *m*/*z*: calcd for $C_{47}H_{85}N_3O_3$: 739.6591 [M^+]; found: 762.6243 [M^++Na]; elemental analysis calcd (%) for $C_{47}H_{85}N_3O_3$: C 76.26, H 11.57, N 5.68; found: C 76.45, H 11.73, N 5.8.

Data for 4: $[\alpha]_D^{20} = -21.2°$ ($c = 5.0$ in $CHCl_3$); ^{1}H NMR (300 MHz, $CDCl_3$, 25 °C, TMS): $\delta = 7.3$–7.17 (m, 5H), 6.61–6.58 (d, 1H), 6.16–6.14 (d, 1H), 5.98 (br, 1H), 4.76–4.69 (m, 1H), 4.18–4.12 (m, 1H), 3.26–3.17 (m, 2H), 3.14–3.0 (m, 2H), 2.16 (t, 2H), 1.55–1.47 (br, 5H), 1.26 (br, 50H), 0.9–0.82 (m, 9H),0.72–0.68 ppm (m, 3H); ESI-MS: *m*/*z*: calcd for $C_{46}H_{83}N_3O_3$: 725.6434 [M^+]; found: 748.6364 [M^++Na]; elemental analysis calcd (%) for $C_{46}H_{83}N_3O_3$: C 76.08, H 11.52, N 5.79; found: C 76.18, H 11.35, N 5.62.

Data for 5: $[\alpha]_D^{20} = -18.8°$ ($c = 4.3$ in $CHCl_3$); ^{1}H NMR (300 MHz, $CDCl_3$, 25 °C, TMS): $\delta = 7.29$–7.12 (m, 5H), 6.39–6.37 (d, 1H), 5.92–5.9 (d, 1H), 5.8 (br, 1H), 4.66–4.59 (m, 1H), 4.31–4.24 (m, 1H), 3.12–3.09 (m, 2H), 3.03–2.94 (m, 2H), 2.04 (t, 2H), 1.53–1.48 (br, 2H), 1.39–1.17 (br, 55H), 0.88–0.86 ppm (m, 6H); ESI-MS: *m*/*z*: calcd for $C_{44}H_{79}N_3O_3$: 697.6121 [M^+]; found: 720.3260 [M^++Na]; elemental analysis calcd (%) for $C_{44}H_{79}N_3O_3$: C 75.70, H 11.41, N 6.02; found: C 75.62, H 11.61, N 5.88.

Data for 6: $[\alpha]_D^{20} = -9.1°$ ($c = 4.2$ in $CHCl_3$); ^{1}H NMR (300 MHz, $CDCl_3$, 25 °C, TMS): $\delta = 7.3$–7.17 (m, 5H), 6.72–6.7 (m, 1H), 6.32 (s, 1H), 6.16–6.14 (br, 1H), 4.62–4.55 (m, 1H), 3.95–3.72 (m, 2H), 3.21–3.12 (m, 2H), 3.10–2.98 (m, 2H), 2.15 (t, 2H), 1.53–1.46 (br, 4H), 1.25 (br, 50H), 0.89–0.85 ppm (m, 6H); ESI-MS: *m*/*z*: calcd for $C_{43}H_{77}N_3O_3$: 683.5965 [M^+]; found: 706.2710 [M^++Na]; elemental analysis calcd (%) for $C_{43}H_{77}N_3O_3$: C 75.50, H 11.35, N 6.14; found: C 75.33, H 11.54, N 5.95.

Data for 7: $[\alpha]_D^{20} = -27.3°$ ($c = 3.0$ in $CHCl_3$); ^{1}H NMR (300 MHz, $CDCl_3$, 25 °C, TMS): $\delta = 8.14$ (s, 1H), 7.71–7.76 (m, 1H), 7.38–7.35 (d, 1H), 7.21–7.08 (m, 3H), 6.14 (br, 2H), 5.92 (br, 1H), 4.67 (br, 1H), 4.28 (br, 1H), 3.49–3.28 (m, 2H), 3.13–3.12 (m, 2H), 2.17 (br, 2H), 1.42–1.25 (br, 54H), 1.01–0.99 (d, 3H), 0.87–0.81 ppm (m, 6H); ESI-MS: *m*/*z*: calcd for $C_{46}H_{80}N_4O_3$: 736.6230 [M^+]; found: 759.5133 [M^++Na]; elemental analysis calcd (%) for $C_{46}H_{80}N_4O_3$: C 74.95, H 10.94, N 7.60; found: C 75.02, H 11.01, N 7.52.

Data for 8: $[\alpha]_D^{20} = -27.1°$ ($c = 2.1$ in $CHCl_3$); ^{1}H NMR (300 MHz, $CDCl_3$, 25 °C, TMS): $\delta = 8.09$ (s, 1H), 7.68–7.65 (d, 1H), 7.38–7.36 (d, 1H), 7.22–7.07 (m, 3H), 6.60–6.57 (d, 1H), 5.85 (t, 1H), 5.67–5.65 (d, 1H), 4.68–4.66 (m, 1H), 4.33–4.29 (m, 1H), 3.51–3.40 (m, 2H), 3.12–3.08 (m, 2H), 2.32 (t, 2H), 1.58–1.10 (br, 57H), 0.9–0.79 ppm (m, 6H); ESI-MS: *m*/*z*: calcd for $C_{46}H_{80}N_4O_3$: 736.6230 [M^+]; found: 759.6761 [M^++Na]; elemental analysis calcd (%) for $C_{46}H_{80}N_4O_3$: C 74.95, H 10.94, N 7.60; found: C 74.78, H 11.05, N 7.71.

Data for 9: $[\alpha]_D^{20} = -36.2°$ ($c = 0.3$ in $CHCl_3$); ^1H NMR (300 MHz, $CDCl_3$, 25 °C, TMS): $\delta = 6.55$ (d, 1H), 6.07 (m, 1H), 5.92 (m, 1H), 4.44–4.35 (m, 2H), 3.24–3.22 (m, 2H), 2.20 (t, 2H), 1.42–1.36 (br, 4H), 1.25–1.0 (br, 56H), 0.87–0.81 ppm (m, 6H); ESI-MS: m/z: calcd for $C_{38}H_{75}N_3O_3$: 621.5808 [M^+]; found: 644.7770 [M^++Na]; elemental analysis calcd (%) for $C_{38}H_{75}N_3O_3$: C 73.37, H 12.15, N 6.76; found: C 73.52, H 12.04, N 6.88.

Data for 5a: $[\alpha]_D^{20} = -14.7°$ ($c = 5.1$ in $CHCl_3$); ^1H NMR (300 MHz, $CDCl_3$, 25 °C, TMS): $\delta = 7.32–7.17$ (m, 5H), 6.43 (br, 1H), 6.0 (br, 2H), 4.65 (br, 1H), 4.37–4.33 (m, 1H), 3.51–3.46 (m, 2H), 3.20–3.05 (m, 2H), 2.16 (t, 2H), 1.50–1.43 (br, 2H), 1.32–1.21 (br, 51H), 0.9–0.79 ppm (m, 6H); ESI-MS: m/z: calcd for $C_{42}H_{75}N_3O_3$: 669.5808 [M^+]; found: 692.5522 [M^++Na]; elemental analysis calcd (%) for $C_{42}H_{75}N_3O_3$: C 75.28, H 11.28, N 6.27; found: C 75.12, H 11.31, N 6.28.

Data for 5b: $[\alpha]_D^{20} = -13.2°$ ($c = 6$ in $CHCl_3$); ^1H NMR (300 MHz, $CDCl_3$, 25 °C, TMS): $\delta = 7.32–7.17$ (m, 5H), 6.31 (br, 1H), 5.95 (br, 2H), 4.63–4.31 (m, 1H), 4.36–4.32 (m, 1H), 3.20–3.15 (m, 2H), 3.07–3.05 (m, 2H), 2.16 (t, 2H), 1.57–1.45 (br, 4H), 1.32–1.18 (br, 45H), 0.9–0.85 ppm (m, 6H); ESI-MS: m/z: calcd for $C_{40}H_{71}N_3O_3$: 641.5495 [M^+]; found: 664.5763 [M^++Na]; elemental analysis calcd (%) for $C_{40}H_{71}N_3O_3$: C 74.83, H 11.15, N 6.55; found: C 74.92, H 11.31, N 6.44.

Data for 5c: $[\alpha]_D^{20} = -7.3°$ ($c = 4.2$ in $CHCl_3$); ^1H NMR (300 MHz, $CDCl_3$, 25 °C, TMS): $\delta = 7.32–7.17$ (m, 5H), 6.34–6.32 (m, 1H), 5.96–5.94 (m, 2H), 4.64–4.61 (m, 1H), 4.36–4.31 (m, 1H), 3.2–3.13 (m, 2H), 3.07–3.05 (m, 2H), 2.16 (t, 2H), 1.47–1.45 (br, 2H), 1.31–1.18 (br, 51H), 0.89–0.81 ppm (m, 6H); ESI-MS: m/z: calcd for $C_{42}H_{75}N_3O_3$: 669.5808 [M^+]; found: 692.6229 [M^++Na]; elemental analysis calcd (%) for $C_{42}H_{75}N_3O_3$: C 75.28, H 11.28, N 6.27; found: C 75.15, H 11.41, N 6.18.

Data for 5d: $[\alpha]_D^{20} = -13.8°$ ($c = 6.1$ in $CHCl_3$); ^1H NMR (300 MHz, $CDCl_3$, 25 °C, TMS): $\delta = 7.28–7.16$ (m, 5H), 6.63–6.61 (m, 1H), 6.43 (br, 1H), 6.14–6.10 (m, 1H), 4.72–4.65 (m, 1H), 4.39–4.30 (m, 1H), 3.18–3.10 (m, 2H), 3.07–2.96 (m, 2H), 2.16 (t, 2H), 1.54–1.45 (br, 4H), 1.31–1.14 (br, 45H), 0.87–0.85 ppm (m, 6H); ESI-MS: m/z: calcd for $C_{40}H_{71}N_3O_3$: 641.5495 [M^+]; found: 664.5623 [M^++Na]; elemental analysis calcd (%) for $C_{40}H_{71}N_3O_3$: C 74.83, H 11.15, N 6.55; found: C 75.02, H 11.33, N 6.43.

Data for 5e: $[\alpha]_D^{20} = -9.5°$ ($c = 4.8$ in $CHCl_3$); ^1H NMR (300 MHz, $CDCl_3$, 25 °C, TMS): $\delta = 7.32–7.17$ (m, 5H), 6.41–6.34 (m, 1H), 6.09–6.07 (d, 1H), 6.0–6.98 (m, 1H), 4.68–4.63 (m, 1H), 4.37–4.29 (m, 1H), 3.18–3.16 (m, 2H), 3.11–2.97 (m, 2H), 2.16 (t, 2H), 1.55–1.46 (br, 2H), 1.32–1.14 (br, 43H), 0.9–0.85 ppm (m, 6H); ESI-MS: m/z: calcd for $C_{38}H_{67}N_3O_3$: 613.5182 [M^+]; found: 636.5011 [M^++Na]; elemental analysis calcd (%) for $C_{38}H_{67}N_3O_3$: C 74.34, H 11.00, N 6.84; found: C 74.18, H 11.13, N 6.93.

Data for 5f: $[\alpha]_D^{20} = -10.2°$ ($c = 3.8$ in $CHCl_3$); ^1H NMR (300 MHz, $CDCl_3$, 25 °C, TMS): $\delta = 7.30–7.15$ (m, 5H), 6.38–6.36 (d, 1H), 5.98–5.96 (m, 2H), 4.63–4.58 (m, 1H), 4.35–4.30 (m, 1H), 3.17–3.11 (m, 2H), 3.05–2.03 (m, 2H), 2.14 (t, 2H), 1.52–1.43 (br, 2H), 1.29–1.23 (br, 47H), 0.87–0.79 ppm (m, 6H); ESI-MS: m/z: calcd for $C_{40}H_{71}N_3O_3$: 641.5495 [M^+]; found: 664.5763 [M^++Na]; elemental analysis calcd (%) for $C_{40}H_{71}N_3O_3$: C 74.83, H 11.15, N 6.55; found: C 74.65, H 11.02, N 6.61.

Data for 5g: $[\alpha]_D^{20} = -8.3°$ ($c = 6.1$ in $CHCl_3$); ^1H NMR (300 MHz, $CDCl_3$, 25 °C, TMS): $\delta = 7.29–7.15$ (m, 5H), 6.42 (br, 1H), 6.0 (br, 2H), 4.65–4.6 (m, 1H), 4.35–4.31 (m, 1H), 3.17–3.11 (m, 2H), 3.05–3.02 (m, 2H), 2.14 (t, 2H), 1.52–1.43 (br, 2H), 1.3–1.23 (br, 43H), 0.87–0.83 ppm (m, 6H); ESI-MS: m/z: calcd for $C_{38}H_{67}N_3O_3$: 613.5182 [M^+]; found: 636.7026 [M^++Na]; elemental analysis calcd (%) for $C_{38}H_{67}N_3O_3$: C 74.34, H 11.00, N 6.84; found: C 74.12, H 11.15, N 6.73.

Data for 5h: $[\alpha]_D^{20} = -7.8°$ ($c = 4.5$ in $CHCl_3$); ^1H NMR (300 MHz, $CDCl_3$, 25 °C, TMS): $\delta = 7.32–7.17$ (m, 5H), 6.33–6.31 (d, 1H), 6.95–5.93 (m, 2H), 4.63–4.59 (m, 1H), 4.36–4.31 (m, 1H), 3.2–3.13 (m, 2H), 3.07–2.05 (m, 2H), 2.16 (t, 2H), 1.47–1.45 (br, 2H), 1.31–1.18 (br, 39H), 0.89–0.81 ppm (m, 6H); ESI-MS: m/z: calcd for $C_{36}H_{63}N_3O_3$: 585.4869 [M^+]; found: 608.1541 [M^++Na]; elemental analysis calcd (%) for $C_{36}H_{63}N_3O_3$: C 73.80, H 10.84, N 7.17; found: C 74.04, H 11.03, N 7.09.

Preparation of the organogels: Required amounts of the compounds were added in 1 mL of organic solvent to a screw-capped vial with internal diameter (i.d.) of 10 mm and slowly heated until the solid was completely dissolved. Then the solutions were cooled (undisturbed) to RT. After 1 h, a colorless and transparent gel was obtained that was verified as stable by inversion of the glass vial.

Determination of gel–sol transition temperature (T_{gel}): The gel-to-sol transition temperature (T_{gel}) was determined by placing the organogel-containing inverted screw-capped glass vial (i.d. of 10 mm) into a thermostatted oil bath and raising the temperature at a rate of 2 °C min^{-1}. The T_{gel} was defined as the temperature (±0.5 °C) at which the gel melted and showed gravitational flow.

Differential scanning calorimetry: Differential scanning calorimetry (DSC) was carried out by using a Perkin–Elmer Diamond DSC. A volume of 40 μL of gelator **5** (0.70 %, w/v) in hot toluene was placed into a large volume capsule (LVC) that was then sealed. The sample LVC pan was placed into the DSC apparatus together with an empty LVC pan as reference. The pans were cooled to 10 °C, and aged for 30 min at this temperature. Heating and cooling scans were then recorded from 10–70 °C at a scan rate of 1 °C min^{-1}.

Microscopy studies: Scanning electron microscopy (SEM) and transmission electron microscopy (TEM) measurements were performed using JEOL-6700F and JEOL JEM 2010 microscopes, respectively. A piece of gel was mounted on a glass slide or 300-mesh carbon-coated copper grid for SEM and TEM sampling, respectively, and dried for a few hours under vacuum before imaging. The morphology of the dried gels of **5** was studied by using atomic force microscopy (AFM, Veeco, modelAP0100) in noncontact mode. A piece of gel was mounted on a silicon wafer and dried for a few hours under vacuum before imaging.

NMR measurements: ^1H NMR was recorded on an AVANCE 300 MHz (Bruker) spectrometer at 1 % (w/v, in C_6D_6) of **5** at variable temperature.

FTIR measurements: FTIR measurements of the gelators **1**–**6** and **5a**–**5h** in $CHCl_3$ solution and dried gel from toluene were carried out in a Nicolet Magna IR-750-series-II spectrophotometer using a 1-mm KBr cell and KBr pellet, respectively, at the minimum gelation concentration.

Fluorescence spectroscopy: The emission spectra of ANS were recorded by using a Varian Cary Eclipse luminescence spectrometer by adding the probe molecules to toluene solutions of gelators **5**, **5d**, and **5h** at various concentrations at RT. ANS was initially dissolved in MeOH to form a 0.002 M superstock solution. This solution was then diluted ten times with toluene to form a 0.0002 M solution. In each experiment, 20 μL of this solution was added to 380 μL of a sample solution in toluene. The final concentration of ANS in the cuvette was 1×10^{-5} M. The ANS solutions were excited at $\lambda_{ex} = 360$ nm.

Dye adsorption: The maximum amount of dye adsorption was monitored by adding 7 mL of dye (0.1 mM) to a sample tube together with 10 mg of xerogels. This solution was left for 24 h at RT to adsorb the dye. The final concentration of the dye in the solution was determined by UV/Vis spectroscopy. A time-dependent study of the adsorption of dyes was carried out with 7 mL of a 0.01-mM dye solution (to avoid the off-scale adsorbance intensity) in the presence of 10 mg of xerogel.

Acknowledgements

P.K.D. is thankful to the Department of Science and Technology, India for financial assistance through a Ramanna Fellowship (No. SR/S1/RFPC-04/2006). S.D., A.S., and S.D. acknowledge the Council of Scientific and Industrial Research, India for their Research Fellowships.

[1] a) P. Terech, R. G. Weiss, *Chem. Rev.* **1997**, *97*, 3133–3159; b) J. H. van Esch, B. L. Feringa, *Angew. Chem.* **2000**, *112*, 1351–1354; *Angew. Chem. Int. Ed.* **2000**, *112*, 2263–2266; c) D. J. Abdallah, R. G. Weiss, *Adv. Mater.* **2000**, *12*, 1237–1247; d) M. George, R. G. Weiss, *Acc. Chem. Res.* **2006**, *39*, 489–497.

[2] a) L. A. Estroff, A. D. Hamilton, *Angew. Chem.* **2000**, *112*, 3589–3592; *Angew. Chem. Int. Ed.* **2000**, *39*, 3447–3450; b) K. Hanabusa,

A. Itoh, M. Kimura, H. Shirai, *Chem. Lett.* **1999**, 767–768; c) F. M. Menger, K. L. Caran, *J. Am. Chem. Soc.* **2000**, *122*, 11679–11691; d) K. Hanabusa, H. Nakayama, M. Kimura, H. Shirai, *Chem. Lett.* **2000**, 1070–1071; e) H. M. Willemen, T. Vermonden, A. T. M. Marcelis, E. J. R. Sudhölter, *Eur. J. Org. Chem.* **2001**, 2329–2335; f) X. Luo, B. Lin, Y. Liang, *Chem. Commun.* **2001**, 1556–1557; g) A. Dasgupta, R. N. Mitra, S. Roy, P. K. Das, *Chem. Asian J.* **2006**, *1*, 780–788.

[3] a) J. Makarević, M. Kokić, B. Perić, V. Tomišić, B. Kojić-Prodić, M. Žinić, *Chem. Eur. J.* **2001**, *7*, 3328–3341; b) J. Becerril, M. I. Burguete, B. Escuder, S. V. Luis, J. F. Miravet, M. Querol, *Chem. Commun.* **2002**, 738–739; c) M. Jokic, J. Makarevic, M. Zinic, *J. Chem. Soc. Chem. Commun.* **1995**, 1723–1724; d) H. T. Stock, N. J. Turner, R. J. McCague, *J. Chem. Soc. Chem. Commun.* **1995**, 2063–2064; e) M. Suzuki, T. Sato, A. Kurose, H. Shirai, K. Hanabusa, *Tetrahedron Lett.* **2005**, *46*, 2741–2745; f) M. Suzuki, S. Owa, M. Kimura, A. Kurose, H. Shiraib, K. Hanabusa, *Tetrahedron Lett.* **2005**, *46*, 303–306; g) S. Roy, D. Das, A. Dasgupta, R. N. Mitra, P. K. Das, *Langmuir* **2005**, *21*, 10398–10404; h) S. Roy, P. K. Das, *Biotechnol. Bioeng.* **2008**, *100*, 756–764.

[4] a) O. Gronwald, S. Shinkai, *Chem. Eur. J.* **2001**, *7*, 4329–4334; b) A. Friggeri, O. Gronwald, K. J. C. van Bommel, S. Shinkai, D. N. Reinhoudt, *J. Am. Chem. Soc.* **2002**, *124*, 10754–10758; c) S. Kiyonaka, S. Shinkai, I. Hamachi, *Chem. Eur. J.* **2003**, *9*, 976–983.

[5] T. Nakashima, N. Kimizuka, *Adv. Mater.* **2002**, *14*, 1113–1116.

[6] a) Y.-C. Lin, B. Kachar, R. G. Weiss, *J. Am. Chem. Soc.* **1989**, *111*, 5542–5551; b) K. Murata, M. Aoki, T. Suzuki, T. Harada, H. Kawabata, T. Komori, F. Ohseto, K. Ueda, S. Shinkai, *J. Am. Chem. Soc.* **1994**, *116*, 6664–6676.

[7] a) M. de Loos, J. H. van Esch, R. M. Kellogg, B. L. Feringa, *Angew. Chem.* **2001**, *113*, 633–636; *Angew. Chem. Int. Ed.* **2001**, *40*, 613–616; b) M. George, R. G. Weiss, *Langmuir* **2002**, *18*, 7124–7135; c) J. J. van Gorp, J. A. J. M. Vekemans, E. W. Meijer, *J. Am. Chem. Soc.* **2002**, *124*, 14759–14769; d) R. P. Lyon, W. M. Atkins, *J. Am. Chem. Soc.* **2001**, *123*, 4408–4413; e) A. Ajayaghosh, S. J. George, *J. Am. Chem. Soc.* **2001**, *123*, 5148–5149; f) G. Wang, A. D. Hamilton, *Chem. Eur. J.* **2002**, *8*, 1954–1961; g) M. George, S. L. Snyder, P. Terech, C. L. Glinka, R. G. Weiss, *J. Am. Chem. Soc.* **2003**, *125*, 10275–10283; h) N. Mohmeyer, D. Kuang, P. Wang, H. W. Schmidt, S. M. Zakeeruddin, M. Gratzel, *J. Mater. Chem.* **2006**, *16*, 2978–2983; i) A. M. Bieser, J. C. Tiller, *Chem. Commun.* **2005**, 3942–3944.

[8] a) N. M. Sangeetha, U. Maitra, *Chem. Soc. Rev.* **2005**, *34*, 821–836; b) M. Suzuki, Y. Sakakibara, S. Kobayashi, M. Kimura, H. Shirai, K. Hanabusa, *Polym. J.* **2002**, *34*, 474–477; c) R. J. H. Hafkamp, B. P. A. Kokke, I. M. Danke, H. P. M. Geurts, A. E. Rowan, M. C. Feiters, R. J. M. Nolte, *Chem. Commun.* **1997**, 545–546; d) Y. Ono, K. Nakashima, M. Sano, Y. Kanekiyo, K. Inoue, J. Hojo, S. Shinkai, *Chem. Commun.* **1998**, 1477–1478; e) J. H. Jung, H. Kobayashi, M. Masuda, T. Shimizu, S. Shinkai, *J. Am. Chem. Soc.* **2001**, *123*, 8785–8789; f) E. D. Sone, E. R. Zubarev, S. I. Stupp, *Angew. Chem.* **2002**, *114*, 1781–1785; *Angew. Chem. Int. Ed.* **2002**, *41*, 1705–1709.

[9] a) S. Kobayashi, N. Hamasaki, M. Suzuki, M. Kimura, H. Shinkai, K. Hanabusa, *J. Am. Chem. Soc.* **2002**, *124*, 6550–6551; b) C. Zhan, J. Wang, J. Yuan, H. Gong, Y. Liu, M. Liu, *Langmuir* **2003**, *19*, 9440–9445; c) S. Kobayashi, K. Hanabusa, N. Hamasaki, M. Kimura, H. Shirai, S. Shinkai, *Chem. Mater.* **2000**, *12*, 1523–1525; d) F. S. Schoonbeek, J. H. van Esch, B. Wagewijs, D. B. A. Rep, M. P. de Haas, T. M. Klapwijk, R. M. Kellog, B. L. Feringa, *Angew. Chem.* **1999**, *111*, 1486–1490; *Angew. Chem. Int. Ed.* **1999**, *38*, 1393–1397; e) F. Placin, J.-P. Desvergne, J.-C. Lassegues, *Chem. Mater.* **2001**, *13*, 117–121; f) A. Shumburo, M. C. Biewer, *Chem. Mater.* **2002**, *14*, 3745–3750; g) G. M. Whitesides, J. P. Mathias, C. T. Seto, *Science* **1991**, *254*, 1312–1319.

[10] S. Bhattacharya, Y. K. Ghosh, *Chem. Commun.* **2001**, 185–186.

[11] a) T. Polubesova, S. Nir, D. Zakada, O. Rabinovitz, C. Serban, L. Groisman, B. Rubin, *Environ. Sci. Technol.* **2005**, *39*, 2343–2348; b) R. Denoyel, E. S. Rey, *Langmuir* **1998**, *14*, 7321–7323; c) A. Sayari, S. Hamoudi, Y. Yang, *Chem. Mater.* **2005**, *17*, 212–216; d) M. Arkas, D. Tsiourvas, C. M. Paleos, *Chem. Mater.* **2005**, *17*, 3439–3444; e) P. Kofinas, D. R. Kioussis, *Environ. Sci. Technol.* **2003**, *37*, 423–427; f) V. Bekiari, P. Lianos, *Chem. Mater.* **2006**, *18*, 4142–4146; g) S. Ray, A. K. Das, A. Banerjee, *Chem. Mater.* **2007**, *19*, 1633–1639; h) E. J. Cho, I. Y. Jeong, S. J. Lee, W. S. Han, J. K. Kang, J. H. Jung, *Tetrahedron Lett.* **2008**, *49*, 1076–1079.

[12] a) N. Mohmeyer, H. W. Schmidt, *Chem. Eur. J.* **2005**, *11*, 863–872; b) M. Suzuki, M. Nanbu, M. Yumoto, H. Shiraib, K. Hanabusa, *New J. Chem.* **2005**, *29*, 1439–1444; c) M. Suzuki, T. Nigawara, M. Yumoto, M. Kimura, H. Shirai, K. Hanabusa, *Org. Biomol. Chem.* **2003**, *1*, 4124–4131; d) H. Yang, T. Yi, Z. Zhou, Y. Zhou, J. Wu, M. Xu, F. Li, C. Huang, *Langmuir* **2007**, *23*, 8224–8230; e) M. Suzuki, T. Sato, H. Shiraib, K. Hanabusa, *New J. Chem.* **2006**, *30*, 1184–1191; f) N. Mohmeyer, H. W. Schmidt, *Chem. Eur. J.* **2007**, *13*, 4499–4509; g) M. Suzuki, Y. Nakajima, M. Yumoto, M. Kimura, H. Shirai, K. Hanabusa, *Org. Biomol. Chem.* **2004**, *2*, 1155–1159.

[13] a) S. Roy, A. Dasgupta, P. K. Das, *Langmuir* **2007**, *23*, 11769–11776; b) A. Shome, S. Debnath, P. K. Das, *Langmuir* **2008**, *24*, 4280–4288.

[14] a) D. Das, A. Dasgupta, S. Roy, R. N. Mitra, S. Debnath, P. K. Das, *Chem. Eur. J.* **2006**, *12*, 5068–5074; b) J. C. Tiller, *Angew. Chem.* **2003**, *115*, 3180–3183; *Angew. Chem. Int. Ed.* **2003**, *42*, 3072–3075.

[15] R. N. Mitra, D. Das, S. Roy, P. K. Das, *J. Phys. Chem. B* **2007**, *111*, 14107–14113.

[16] M. Suzuki, M. Yumoto, M. Kimura, H. Shiraib, K. Hanabusa, *Chem. Commun.* **2002**, 884–885.

[17] R. Scartazzini, P. L. Luisi, *J. Phys. Chem.* **1988**, *92*, 829–833.

[18] J. L. Pozzo, G. M. Clavier, J. P. Desvergne, *J. Mater. Chem.* **1998**, *8*, 2575–2577.

[19] a) M. Moniruzzaman, P. R. Sundararajan, *Langmuir* **2005**, *21*, 3802–3807; b) Y. Li, K. Liu, J. Liu, J. Peng, X. Feng, Y. Fang, *Langmuir* **2006**, *22*, 7016–7020.

[20] a) J. Brinksma, B. L. Feringa, R. M. Kellogg, R. Vreeker, J. H. van Esch, *Langmuir* **2000**, *16*, 9249–9255; b) A. Pal, Y. K. Ghosh, S. Bhattacharya, *Tetrahedron* **2007**, *63*, 7334–7348.

[21] M. Suzuki, Y. Nakajima, M. Yumoto, M. Kimura, H. Shirai, K. Hanabusa, *Langmuir* **2003**, *19*, 8622–8624.

[22] a) G. John, J. H. Jung, M. Masuda, T. Shimizu, *Langmuir* **2004**, *20*, 2060–2065; b) C. Wang, D. Zhang, D. Zhu, *Langmuir* **2007**, *23*, 1478–1482; c) A. M. Bieser, J. C. Tiller, *J. Phys. Chem. B* **2007**, *111*, 13180–13187.

[23] L. Su, C. Bao, R. Lu, Y. Chen, T. Xu, D. Song, C. Tan, T. Shi, Y. Zhao, *Org. Biomol. Chem.* **2006**, *4*, 2591–2594.

[24] a) K. Köhler, G. Förster, A. Hauser, B. Dobner, U. F. Heiser, F. Ziethe, W. Richter, F. Steiniger, M. Drechsler, H. Stettin, A. Blume, *J. Am. Chem. Soc.* **2004**, *126*, 16804–16813; b) M. Kogiso, T. Hanada, K. Yase, T. Shimizu, *Chem. Commun.* **1998**, 1791–7192; c) T. Shimizu, M. Masuda, *J. Am. Chem. Soc.* **1997**, *119*, 2812–2818.

[25] R. Jayakumar, M. Murugesan, C. Asokan, M. A. Scibioh, *Langmuir* **2000**, *16*, 1489–1496.

Received: April 16, 2008
Published online: July 18, 2008

